

# Synthesis and Thermal Properties of Novel Periodic Poly(ester–amide)s Derived from Adipate, Butane-1,4-diamine, and Linear Aliphatic Diols

Hiroaki Tetsuka,<sup>†</sup> Yoshiharu Doi,<sup>‡</sup> and Hideki Abe<sup>\*,†,‡</sup>

Department of Innovative and Engineered Materials, Tokyo Institute of Technology, Nagatsuta, Midori-ku, Yokohama 226-8502, Japan, and Polymer Chemistry Laboratory, RIKEN Institute, Hirosawa, Wako-shi, Saitama 351-0198, Japan

Received December 1, 2005; Revised Manuscript Received February 24, 2006

**ABSTRACT:** Novel aliphatic poly(ester–amide)s with a periodic sequential structure consisting of ester and amide groups were synthesized by two-step polycondensation reactions using adipate, butane-1,4-diamine, and linear diols with different chain lengths, ranging from 3 to 6 methylene groups. Effects of the monomeric structure and sequential length of ester units on the thermal properties and crystalline structure of the obtained periodic copolymers were determined by means of differential scanning calorimetry (DSC) and wide-angle X-ray diffraction (WAXD). On the basis of DSC measurements, the melting temperatures of the periodic copolymers were higher than those of homopolyesters consisting of the same ester units and tended to increase with an increase in amide content. The copolymers from adipate, butane-1,4-diol, and butane-1,4-diamine had especially high thermal stability compared with the poly(tetramethylene adipate) homopolyester, and the melting temperatures detected were above 200 °C. The X-ray diffraction patterns of periodic copolymers were variable with some copolymers displaying patterns similar to homopolyesters while other copolymers had diffraction patterns that were very different than the homopolyester, dependent on both the monomeric structure of the ester units and the sequential length of the ester units. The formation of different chain packing structures compared to homopolyesters induced the remarkable enhancement of thermal stability, suggesting that molecular chain arrangements based on the intermolecular hydrogen bond interactions play a decisive role in the formation of a thermally stable crystalline region of periodic copolymers and that the formation of intermolecular hydrogen bonds is strongly dependent on both the monomeric structure of ester units and the sequential length of ester units. Furthermore, the effects of annealing treatment on the thermal properties and molecular chain arrangements of periodic copolymers were investigated.

## Introduction

The production of polymer materials with excellent physical properties and biodegradability using naturally occurring chemicals, such as dicarboxylic acids, amino acids, hydroxyl acids, and diols, has become an important topic in polymer industry because of the declining amounts of petroleum and environmental issues.<sup>1,2</sup> Aliphatic polyesters can be synthesized by polycondensation reaction or ring-opening polyesterification using the naturally occurring chemicals and their derivatives as building blocks and are currently the most important family of biodegradable polymers. However, in general, their thermal and mechanical properties are not optimal for a wide range of industrial applications. On the other hand, synthetic aliphatic polyamides are generally not biodegradable but have high thermal stability and mechanical properties because of strong intermolecular hydrogen-bond interactions. Combining of the favorable properties of both aliphatic polyesters and polyamides may lead to polymer materials that have both superior physical properties and suitable biodegradability.

So far, many types of aliphatic poly(ester–amide)s have been synthesized by various techniques.<sup>3–26</sup> Katayama et al.<sup>3</sup> synthesized alternating poly(ester–amide)s from adipic acid and *N,N'*-1,4-hexanediylbis(6-hydroxyhexanamide) by melt and solution polycondensation reaction. Tokiwa et al.<sup>4</sup> investigated random poly(ester–amide)s synthesized by amide–ester interchange reactions of nylons and polycaprolactone and showed

that the copolymers were degraded by lipase. Castaldo et al.<sup>5</sup> synthesized block poly(ester–amide) by two-step polycondensation reactions using adipoyl chloride, hexane-1,6-diamine, and decane-1,10-diol. Goodman et al.<sup>6</sup> also synthesized block and random aliphatic poly(ester–amide)s from adipic acid, hexane-1,6-diamine, and butane-1,4-diol. Inata et al.<sup>7</sup> and Seppälä et al.<sup>8</sup> synthesized poly(ester–amide)s using the bisoxazoline group as chain-extender for linear oligoester. From the literature cited above, the thermal and mechanical properties of poly(ester–amide)s showed a strong dependence on both the content and distribution of the amide units in the main chains.

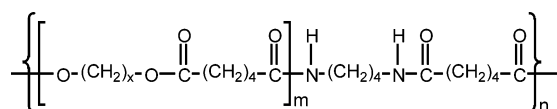
Previously, Abe and Doi synthesized novel biodegradable poly(ester–amide)s with defined periodic sequence consisting of ester and amide units by two-step polycondensation reactions using dimethyl succinate, butane-1,4-diol, and butane-1,4-diamine.<sup>24</sup> The structure, physical properties, and enzymatic degradation of the copolymers were investigated. The melting temperatures of periodic poly(ester–amide)s were much higher than the melting temperature of the homopolyester, and the values varied in a large temperature range dependent on the length of the periodic sequences of the ester and amide units. In addition, the wide-angle X-ray diffraction patterns of the periodic copolymers were very different from the diffraction pattern of the corresponding homopolyester, suggesting that the amide units introduced periodically into the polyester main chains are included in the crystalline region to form a novel crystalline structure. On the basis of the above results, it may be concluded that optimal regulation of the thermal properties is achieved when the crystallizable sequence consisting of both ester and amide units is present with high regularity in the main chain.

\* To whom correspondence should be addressed: e-mail habe@riken.jp; Tel +81-48-467-9404; Fax +81-48-462-4667.

<sup>†</sup> Tokyo Institute of Technology.

<sup>‡</sup> RIKEN Institute.

Scheme 1



**P(tri)1-7** :  $x = 3, m = 2, 3, 4, \dots, 8$

**P(tet)1-6** :  $x = 4, m = 2, 3, 4, \dots, 7$

**P(pen)1-7** :  $x = 5, m = 2, 3, 4, \dots, 8$

**P(hex)1-7** :  $x = 6, m = 2, 3, 4, \dots, 8$

In this work, we synthesized novel periodic poly(ester—amide) series by two-step polycondensation reactions using adipate, butane-1,4-diamine, and aliphatic diols with various chain lengths (Scheme 1) and characterized the structures and thermal properties of the obtained copolymers by NMR spectroscopy, differential scanning calorimetry (DSC), and wide-angle X-ray diffraction (WAXD). The linear aliphatic diols, ranging from 3 to 6 methylene units, were used as comonomers to obtain a fundamental understanding of the influences of both monomeric and sequential structures in this copolymer series on the thermal properties. In addition, the annealing effects on the melting behavior of periodic poly(ester—amide)s were investigated. On the basis of the above results, the relationships among the thermal properties, molecular structures, and crystalline structures in the periodic poly(ester—amide)s are discussed.

## Experimental Part

**Materials.** Basic materials were purchased from Kanto Chemical Co. Phenol, dimethyl adipate, diols (propane-1,3-diol, butane-1,4-diol, pentane-1,5-diol, and hexane-1,6-diol), and butane-1,4-diamine were used as supplied without further purification.

**Synthesis of Diphenyl Adipate.** Diphenyl adipate was prepared by a exchange reaction between phenol and dimethyl adipate in the presence of titanium tetrakisopropoxide ( $\text{Ti}(\text{OiPr})_4$ ) as a catalyst. Phenol (0.64 mol), dimethyl adipate (0.16 mol), and  $\text{Ti}(\text{OiPr})_4$  catalyst (0.40 mmol) were placed into a reactor under a nitrogen atmosphere. The exchange reaction was carried out at 170 °C and at atmospheric pressure for 36 h, after which the methanol was removed by distillation. The temperature was raised to 190 °C, and the pressure was slowly reduced to 1.0 mmHg in order to remove the excess phenol by distillation. The mixture was then cooled to room temperature, and a white powder precipitated. The white powder was washed with diethyl ether and dried under vacuum at room temperature. The product was obtained with a yield of 58%, and the purity, determined by  $^1\text{H}$  NMR, was >97%.

$^1\text{H}$  NMR ( $\text{CDCl}_3$ , TMS, int ref):  $\delta$  7.39 (t, 4H,  $-m\text{-C}_6\text{H}_5$ ), 7.25 (t, 2H,  $-p\text{-C}_6\text{H}_5$ ), 7.07 (d, 4H,  $-o\text{-C}_6\text{H}_5$ ), 2.64 (t, 4H,  $\text{OCOCH}_2$ ), 1.90 (m, 4H,  $\text{OCOCH}_2\text{CH}_2$ ).

**Preparation of Oligoesters with Adipate Methyl Ester End Groups.** Oligoesters of oligomethylene adipate with adipate methyl ester end groups were prepared by the condensation reaction of diol (propane-1,3-diol and butane-1,4-diol) with an excess of dimethyl adipate in the presence of titanium tetrakisopropoxide ( $\text{Ti}(\text{OiPr})_4$ ) as a catalyst. Diol (0.12 mol), dimethyl adipate (0.18 mol), and  $\text{Ti}(\text{OiPr})_4$  catalyst (0.30 mmol) were placed into a reactor under a nitrogen atmosphere. The oligomerization was carried out at 170 °C and at atmospheric pressure for 6 h, and methanol was removed by distillation. The produced oligoesters were dissolved in chloroform and precipitated in cold methanol at 0 °C. The product was dried under vacuum at room temperature.

**Preparation of Oligoesters with Adipate Phenyl Ester End Groups.** Oligoesters of oligomethylene adipate with adipate phenyl ester end groups were prepared by the condensation reaction of diol (propane-1,3-diol, pentane-1,5-diol, and hexane-1,6-diol) with an excess of diphenyl adipate in the presence of titanium tetrakisopropoxide ( $\text{Ti}(\text{OiPr})_4$ ) as a catalyst. Diol (0.04 mol), diphenyl adipate (0.06 mol), and  $\text{Ti}(\text{OiPr})_4$  catalyst (0.01 mmol) were placed into a reactor under a nitrogen atmosphere. First, the oligomerization was carried out at 170 °C and at atmospheric pressure for 4 h.

Then, the pressure was slowly reduced to 1.0 mmHg, and phenol was removed by distillation over a 1 h period. The produced oligoesters were dissolved in chloroform and precipitated in cold methanol at 0 °C. The product was dried under vacuum at room temperature.

**Fractionation of Monodispersed Oligoesters with Symmetric Structure.** Fractionation of monodispersed oligoesters with symmetric structure composed of adipate methyl ester end groups and of adipate phenyl ester end groups was performed on a JASCO supercritical fluid chromatography (SCFC) system with an MD-2010 plus multiwavelength detector. A stainless steel column ( $150 \times 4.6 \text{ mm}^2$ ) containing silica gel (5  $\mu\text{m}$ ) (SFCpak Crest SIL-5; JASCO) or a stainless steel column ( $200 \times 20 \text{ mm}^2$ ) containing silica gel (10–20  $\mu\text{m}$ ) (SFC Megapak SIL(10/20); JASCO) was used for fractionation at 60 °C. A mixture of supercritical carbon dioxide and acetonitrile was applied as eluent, and the pressure of the eluent was regulated at 12 MPa. The flow rate of carbon dioxide was maintained at 4 mL/min, while the rate of acetonitrile was linearly increased for each condition. The oligoesters were detected spectrophotometrically at a wavelength of 210 nm. Each fraction of oligoester was collected from the eluate, and the solvent was evaporated. The purity and structure of each fractionated oligoester were evaluated by  $^1\text{H}$  NMR analysis, MALDI-ToF MS analysis, and the reinjection analysis of oligoesters in SCFC.

Oligo(trimethylene adipate) with adipate methyl ester end groups:  $^1\text{H}$  NMR ( $\text{CDCl}_3$ , TMS, int ref):  $\delta$  4.15 (t,  $\text{OCH}_2\text{CH}_2$ ), 3.67 (s,  $\text{OCH}_3$ ), 2.34 (br t,  $\text{OCOCH}_2\text{CH}_2$ ), 1.97 (br m,  $\text{OCH}_2\text{CH}_2$ ), 1.66 (m,  $\text{OCOCH}_2\text{CH}_2$ ).  $^1\text{H}$  NMR purity (mol %): as lowest values calculated from the ratio of end groups: fraction no. 1 (Om1) >95%, no. 2 (Om2) >96%, no. 3 (Om3) >76%, no. 4 (Om4) >66%, no. 5 (Om5) >60%, no. 6 (Om6) >57%, no. 7 (Om7) >56% (see Figure 1A).

Oligo(tetramethylene adipate) with adipate methyl ester end groups:  $^1\text{H}$  NMR ( $\text{CDCl}_3$ , TMS, int ref):  $\delta$  4.09 (t,  $\text{OCH}_2\text{CH}_2$ ), 3.67 (s,  $\text{OCH}_3$ ), 2.34 (br t,  $\text{OCOCH}_2\text{CH}_2$ ), 1.70 (br m,  $\text{OCH}_2\text{CH}_2$ ), 1.66 (m,  $\text{OCOCH}_2\text{CH}_2$ ).  $^1\text{H}$  NMR purity (mol %): fraction no. 1 >97%, no. 2 >98%, no. 3 >97%, no. 4 >97%, no. 5 >94%, no. 6 >89%.

Oligo(trimethylene adipate) with adipate phenyl ester end groups.  $^1\text{H}$  NMR ( $\text{CDCl}_3$ , TMS, int ref):  $\delta$  7.37 (t,  $-m\text{-C}_6\text{H}_5$ ), 7.24 (t,  $-p\text{-C}_6\text{H}_5$ ), 7.07 (d,  $-o\text{-C}_6\text{H}_5$ ), 4.15 (t,  $\text{OCH}_2\text{CH}_2$ ), 2.59 (t,  $\text{C}_6\text{H}_5\text{OCOCH}_2\text{CH}_2$ ), 2.39 (t,  $\text{C}_6\text{H}_5\text{OCOCH}_2\text{CH}_2\text{CH}_2\text{CH}_2$ ), 2.33 (t,  $\text{OCOCH}_2\text{CH}_2$ ), 1.97 (m,  $\text{OCH}_2\text{CH}_2$ ), 1.78 (m,  $\text{C}_6\text{H}_5\text{OCOCH}_2\text{CH}_2\text{CH}_2\text{CH}_2$ ), 1.66 (m,  $\text{OCOCH}_2\text{CH}_2$ ).  $^1\text{H}$  NMR purity (mol %): fraction no. 1 (Op1) >95%, no. 2 (Op2) >95%, no. 3 (Op3) >96%, no. 4 (Op4) >94%, no. 5 (Op5) >95%, no. 6 (Op6) >96%, no. 7 (Op7) >97% (see Figure 1B).

Oligo(pentamethylene adipate) with adipate phenyl ester end groups:  $^1\text{H}$  NMR ( $\text{CDCl}_3$ , TMS, int ref):  $\delta$  7.37 (t,  $-m\text{-C}_6\text{H}_5$ ), 7.22 (t,  $-p\text{-C}_6\text{H}_5$ ), 7.08 (d,  $-o\text{-C}_6\text{H}_5$ ), 4.06 (t,  $\text{OCH}_2\text{CH}_2\text{CH}_2$ ), 2.59 (t,  $\text{C}_6\text{H}_5\text{OCOCH}_2\text{CH}_2$ ), 2.38 (t,  $\text{C}_6\text{H}_5\text{OCOCH}_2\text{CH}_2\text{CH}_2\text{CH}_2\text{CH}_2$ ), 2.32 (t,  $\text{OCOCH}_2\text{CH}_2$ ), 1.78 (m,  $\text{C}_6\text{H}_5\text{OCOCH}_2\text{CH}_2\text{CH}_2\text{CH}_2\text{CH}_2$ ), 1.65 (m,  $\text{OCH}_2\text{CH}_2\text{CH}_2$  and  $\text{OCOCH}_2\text{CH}_2$ ), 1.41 (m,  $\text{OCH}_2\text{CH}_2\text{CH}_2$ ).  $^1\text{H}$  NMR purity (mol %): fraction no. 1 >93%, no. 2 >94%, no. 3 >97%, no. 4 >94%, no. 5 >94%, no. 6 >91%, no. 7 >90%.

Oligo(hexamethylene adipate) with adipate phenyl ester end groups:  $^1\text{H}$  NMR ( $\text{CDCl}_3$ , TMS, int ref):  $\delta$  7.37 (t,  $-m\text{-C}_6\text{H}_5$ ), 7.22 (t,  $-p\text{-C}_6\text{H}_5$ ), 7.07 (d,  $-o\text{-C}_6\text{H}_5$ ), 4.06 (t,  $\text{OCH}_2\text{CH}_2\text{CH}_2$ ), 2.59 (t,  $\text{C}_6\text{H}_5\text{OCOCH}_2\text{CH}_2$ ), 2.38 (t,  $\text{C}_6\text{H}_5\text{OCOCH}_2\text{CH}_2\text{CH}_2\text{CH}_2\text{CH}_2$ ), 2.32 (t,  $\text{OCOCH}_2\text{CH}_2$ ), 1.78 (m,  $\text{C}_6\text{H}_5\text{OCOCH}_2\text{CH}_2\text{CH}_2\text{CH}_2\text{CH}_2$ ), 1.65 (m,  $\text{OCH}_2\text{CH}_2\text{CH}_2$  and  $\text{OCOCH}_2\text{CH}_2$ ), 1.37 (m,  $\text{OCH}_2\text{CH}_2\text{CH}_2$ ).  $^1\text{H}$  NMR purity (mol %): fraction no. 1 >97%, no. 2 >98%, no. 3 >97%, no. 4 >96%, no. 5 >97%, no. 6 >97%, no. 7 >97%.

**Synthesis of Homopolymers.** Polyesters were synthesized by the condensation reaction of dimethyl adipate with each diol in the presence of titanium tetrakisopropoxide ( $\text{Ti}(\text{OiPr})_4$ ) as a catalyst. Equimolar amounts of dimethyl adipate and diol and  $\text{Ti}(\text{OiPr})_4$  catalyst (0.01 mol %) were placed into a reactor under a nitrogen atmosphere. First, the polymerization was carried out at 170 °C and at atmospheric pressure for 6 h, and methanol was removed by distillation. Then the temperature was increased to 190 °C, and

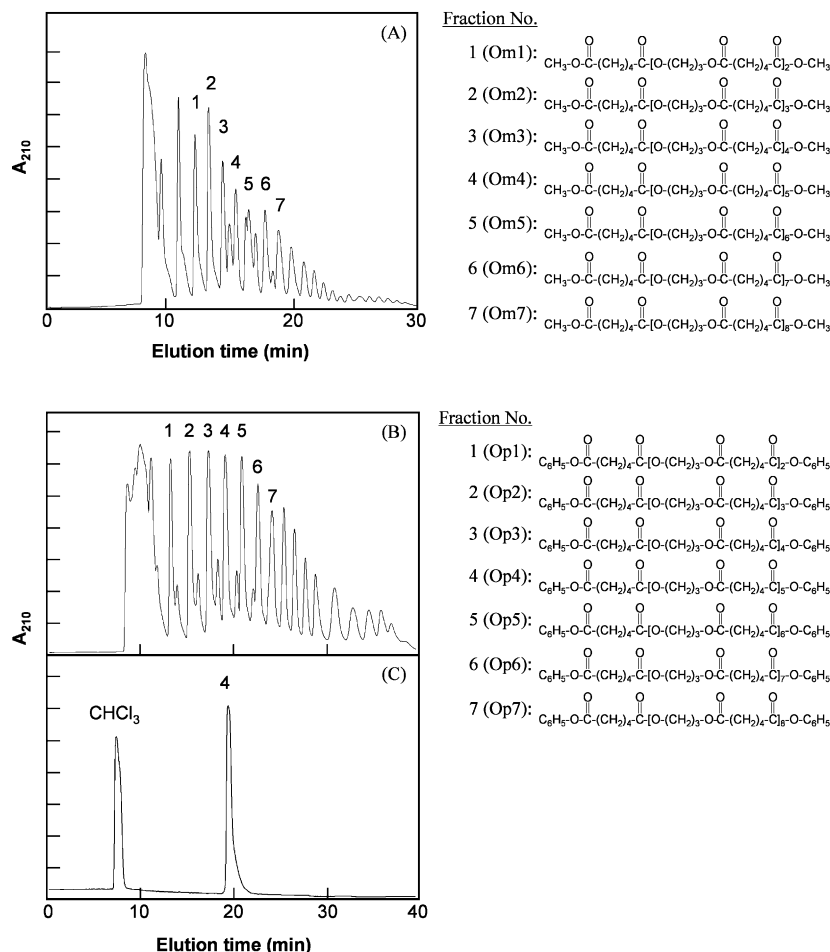


**Figure 1.** SCFC elution profiles of oligomers of trimethylene adipate derived (A) from dimethyl adipate and propane-1,3-diol and (B) from diphenyl adipate and propane-1,3-diol. SCFC reinjection profile (C) of fractionated oligomer of trimethylene adipate (sample Op4).

the pressure was slowly reduced to 0.1 mmHg. After 8 h, the product was cooled to room temperature. The produced polyester was dissolved in chloroform and precipitated in methanol or diethyl ether. The precipitate was dried under vacuum at room temperature.

**Copolymerization of Monodispersed Oligoesters with Butane-1,4-diamine.** Periodic copolymers were synthesized by the condensation reaction between diamine and monodispersed oligoester in the absence of catalyst. Equimolar amounts of monodispersed oligoester and butane-1,4-diamine were admitted into a reactor under nitrogen. The copolymerization was carried out at 120 °C and at atmospheric pressure for 6 h. The products were dissolved in chloroform or trifluoroethanol and precipitated in methanol or diethyl ether. The precipitate was dried under vacuum at room temperature.

Poly(trimethylene adipate-*per*-tetramethylene adipamide):  $^1\text{H}$  NMR ( $\text{CDCl}_3$ , TMS, int ref):  $\delta$  4.15 (t,  $\text{OCH}_2$ ), 3.26 (br q,  $\text{NHCH}_2$ ), 2.33 (br t,  $\text{OCOCH}_2$ ), 2.20 (br t,  $\text{NHCOCH}_2$ ), 1.97 (br m,  $\text{OCH}_2\text{CH}_2$ ), 1.66 (br m,  $\text{OCOCH}_2\text{CH}_2$  and  $\text{NHCOCH}_2\text{CH}_2$ ), 1.54 (br m,  $\text{NHCH}_2\text{CH}_2$ ).  $^{13}\text{C}$  NMR ( $\text{CDCl}_3$ , TMS, int ref):  $\delta$  173.45 (NHCO), 173.21–172.7 (OCO), 60.94 ( $\text{OCH}_2$ ), 39.02 ( $\text{NHCH}_2$ ), 36.26 ( $\text{NHCOCH}_2$ ), 33.78 ( $\text{OCOCH}_2$ ), 27.97 ( $\text{OCH}_2\text{CH}_2$ ), 26.94 ( $\text{NHCH}_2\text{CH}_2$ ), 25.13 ( $\text{NHCOCH}_2\text{CH}_2$ ), 24.32 ( $\text{OCOCH}_2\text{CH}_2$ ).

Poly(tetramethylene adipate-*per*-tetramethylene adipamide):  $^1\text{H}$  NMR ( $\text{CDCl}_3$ , TMS, int ref):  $\delta$  4.09 (t,  $\text{OCH}_2$ ), 3.26 (br q,  $\text{NHCH}_2$ ), 2.33 (br t,  $\text{OCOCH}_2$ ), 2.20 (br t,  $\text{NHCOCH}_2$ ), 1.70 (br m,  $\text{OCH}_2\text{CH}_2$ ), 1.66 (br m,  $\text{OCOCH}_2\text{CH}_2$  and  $\text{NHCOCH}_2\text{CH}_2$ ), 1.53 (br m,  $\text{NHCH}_2\text{CH}_2$ ).  $^{13}\text{C}$  NMR ( $\text{CDCl}_3$ , TMS, int ref):  $\delta$  173.56 (NHCO), 173.31 (OCO), 63.85 ( $\text{OCH}_2$ ), 39.01 ( $\text{NHCH}_2$ ), 36.26 ( $\text{NHCOCH}_2$ ), 33.86 ( $\text{OCOCH}_2$ ), 26.94 ( $\text{NHCH}_2\text{CH}_2$ ), 25.30 ( $\text{OCH}_2\text{CH}_2$ ), 25.12 ( $\text{NHCOCH}_2\text{CH}_2$ ), 24.38 ( $\text{OCOCH}_2\text{CH}_2$ ).

Poly(pentamethylene adipate-*per*-tetramethylene adipamide):  $^1\text{H}$  NMR ( $\text{CDCl}_3$ , TMS, int ref):  $\delta$  4.07 (t,  $\text{OCH}_2$ ), 3.26 (br q,  $\text{NHCH}_2$ ),

2.35 (br t,  $\text{OCOCH}_2$ ), 2.20 (br t,  $\text{NHCOCH}_2$ ), 1.66 (br m,  $\text{OCH}_2\text{CH}_2$  and  $\text{OCOCH}_2\text{CH}_2$ ), 1.53 (br m,  $\text{NHCH}_2\text{CH}_2$ ), 1.41 (br m,  $\text{OCH}_2\text{CH}_2\text{CH}_2$ ).  $^{13}\text{C}$  NMR ( $\text{CDCl}_3$ , TMS, int ref):  $\delta$  173.61 (NHCO), 173.36–172.73 (OCO), 64.16 ( $\text{OCH}_2$ ), 38.99 ( $\text{NHCH}_2$ ), 36.26 ( $\text{NHCOCH}_2$ ), 33.89 ( $\text{OCOCH}_2$ ), 28.28 ( $\text{OCH}_2\text{CH}_2$ ), 26.94 ( $\text{NHCH}_2\text{CH}_2$ ), 25.12 ( $\text{NHCOCH}_2\text{CH}_2$ ), 24.39 ( $\text{OCOCH}_2\text{CH}_2$ ), 22.44 ( $\text{OCH}_2\text{CH}_2\text{CH}_2$ ).

Poly(hexamethylene adipate-*per*-tetramethylene adipamide):  $^1\text{H}$  NMR ( $\text{CDCl}_3$ , TMS, int ref):  $\delta$  4.06 (t,  $\text{OCH}_2$ ), 3.26 (br q,  $\text{NHCH}_2$ ), 2.33 (br t,  $\text{OCOCH}_2$ ), 2.20 (br t,  $\text{NHCOCH}_2$ ), 1.66 (br m,  $\text{OCH}_2\text{CH}_2$  and  $\text{OCOCH}_2\text{CH}_2$ ), 1.53 (br m,  $\text{NHCH}_2\text{CH}_2$ ), 1.37 (br m,  $\text{OCH}_2\text{CH}_2\text{CH}_2$ ).  $^{13}\text{C}$  NMR ( $\text{CDCl}_3$ , TMS, int ref):  $\delta$  173.66 (NHCO), 173.42 (OCO), 64.31 ( $\text{OCH}_2$ ), 39.00 ( $\text{NHCH}_2$ ), 36.26 ( $\text{NHCOCH}_2$ ), 33.91 ( $\text{OCOCH}_2$ ), 28.52 ( $\text{OCH}_2\text{CH}_2$ ), 26.94 ( $\text{NHCH}_2\text{CH}_2$ ), 25.61 ( $\text{OCH}_2\text{CH}_2\text{CH}_2$ ), 25.13 ( $\text{NHCOCH}_2\text{CH}_2$ ), 24.41 ( $\text{OCOCH}_2\text{CH}_2$ ).

**Compositions of Poly(ester–amide)s.** Compositions of the obtained copolymers were calculated from the  $^1\text{H}$  NMR spectra. The amide fractions (mol %) in the copolymers were determined by integration of the proton resonances of distinct four peaks: (c) (4.06–4.15 ppm:  $\text{OCH}_2$ ), (g) (3.26 ppm:  $\text{NHCH}_2$ ), (a) (2.33–2.35 ppm:  $\text{OCOCH}_2$ ), and (f) (2.20 ppm:  $\text{NHCOCH}_2$ ) (Figures 3 and 4), as in the following two equations:

$$\text{amide mol \%} = \left( \frac{g}{c + g} \right) \times 100\% = \left( \frac{f}{a + f} \right) \times 100\%$$

The calculated values from two equations were in good agreement with each other for any cases.

**Analytical Procedures.**  $^1\text{H}$  NMR analysis of oligoester and poly(ester–amide) samples was performed with a JNM AL-300 spectrometer. The samples (5 mg/mL) were dissolved in either  $\text{CDCl}_3$  or  $\text{CF}_3\text{CD}_2\text{OD}$ , and the 300 MHz  $^1\text{H}$  NMR spectra were

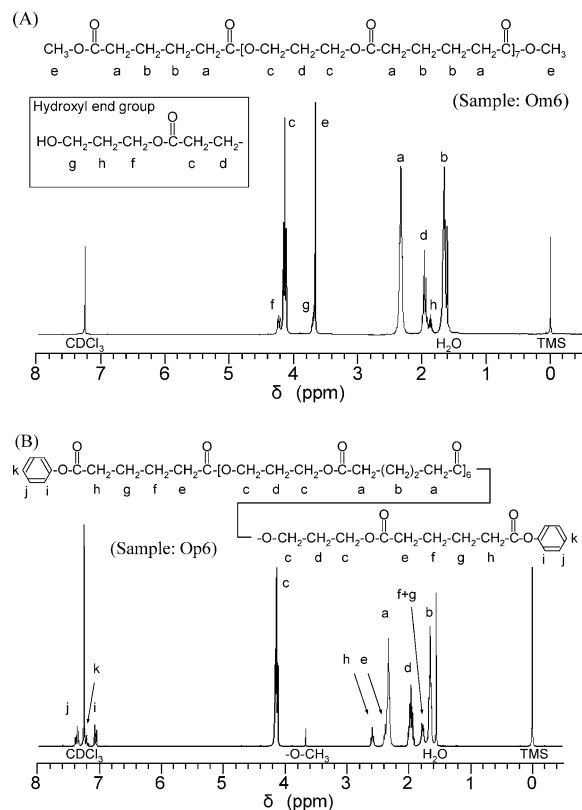


**Figure 2.**  $^1\text{H}$  NMR spectra of fractionated oligomers of trimethylene adipate derived (A) (sample Om6) from dimethyl adipate and propane-1,3-diol and (B) (sample Op6) from diphenyl adipate and propane-1,3-diol.

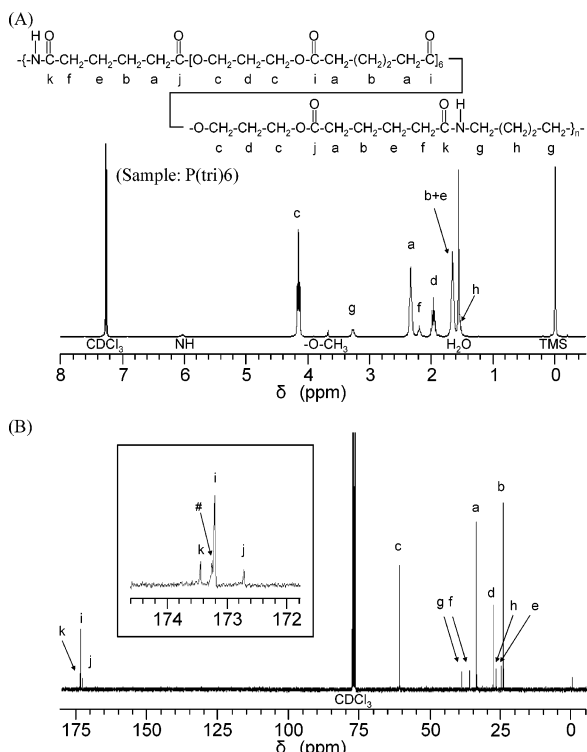


**Figure 3.**  $^1\text{H}$  NMR (A) and  $^{13}\text{C}$  NMR (B) spectra of produced copolymers (sample P(tri)6) from condensation of monodispersed oligomer of trimethylene adipate (sample Op6) and butane-1,4-diamine, (#: from methyl ester or hydroxyl chain end).

recorded at 23 °C with a 6.2  $\mu\text{s}$  pulse width (45° pulse angle), 3 s pulse repetition, 6000 Hz spectroscopic width, and 16K data points.

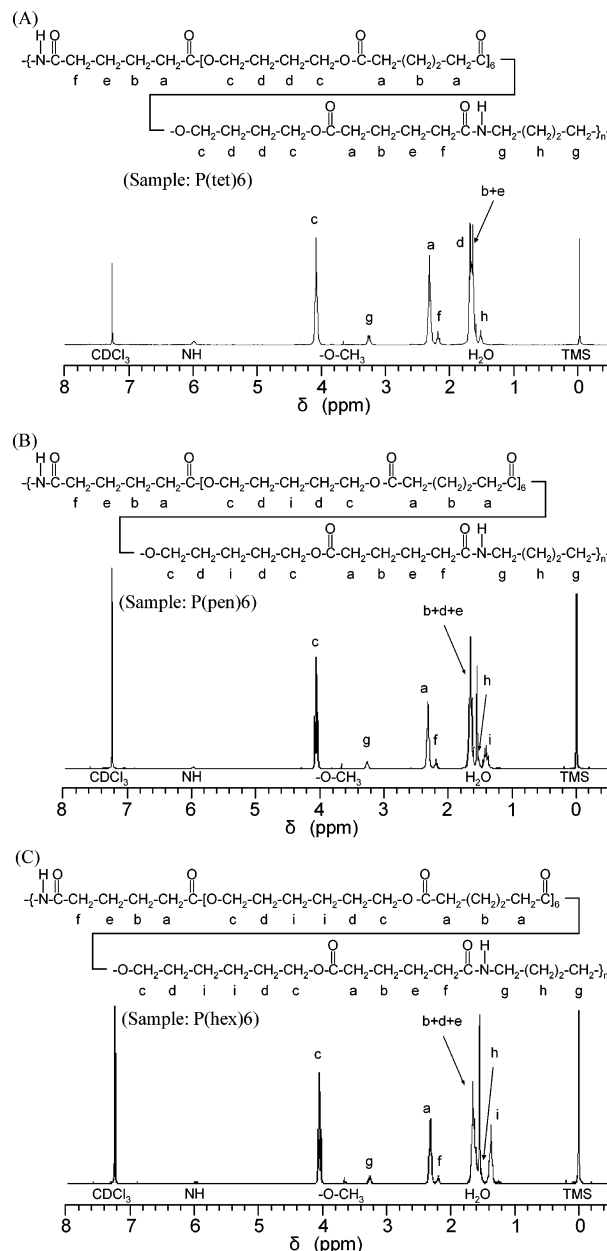


**Figure 4.**  $^1\text{H}$  NMR spectra of produced copolymers (A) (sample P(tet)6), (B) (sample P(pen)6), and (C) (sample P(hex)6) from condensation of each monodispersed oligoester with 7 repeating units and butane-1,4-diamine.

$^{13}\text{C}$  NMR analysis of poly(ester–amide) samples was performed with a JNM AL-300 spectrometer. The samples (30 mg/mL) were dissolved in either  $\text{CDCl}_3$  or  $\text{CF}_3\text{CD}_2\text{OD}$ , and the 75 MHz  $^{13}\text{C}$  NMR spectra were recorded at 23 °C with a 3.8  $\mu\text{s}$  pulse width (45° pulse angle), 1.4 s pulse repetition, 20 000 Hz spectroscopic width, and 32K data points.

MALDI MS data recorded using a time-of-flight MALDI MS spectrometer (Ultraflex, Bruker) with reflector and positive-ion models. Ions were generated using a nitrogen laser operating at wavelength 337 nm. The spectra were obtained from the 250 laser shots accumulated. For the sample preparation, 0.5 mg of 2,5-dihydroxybenzoic acid as the matrix and 10  $\mu\text{L}$  of methanol were added to about 10 mg of the fractionated oligoester samples in 100  $\mu\text{L}$  of tetrahydrofuran. For the analysis, 0.5  $\mu\text{L}$  of the mixed solution was spotted on the sample slide and dried in air.

All molecular weight data were obtained by gel-permeation chromatography at 40 °C, using a Shimadzu 10A GPC system and a 10A refractive index detector with Shodex K-806M and K-802 columns. Chloroform was used as an eluent at a flow rate of 0.8



mL/min, and a sample concentration of 1.0 mg/mL was applied. Polystyrene standards with a low polydispersity were used to make a calibration curves.

Differential scanning calorimetry (DSC) data of polyester and poly(ester–amide) samples were recorded in the temperature range of  $-100$  to  $300$  °C on a Perkin-Elmer Pyris 1 equipped with a cooling accessory under a nitrogen flow of 20 mL/min. Samples of 3–5 mg were encapsulated in aluminum pans and heated at a rate of 20 °C/min. The melting temperature ( $T_m$ ) and enthalpy of fusion ( $\Delta H_m$ ) were determined from the DSC endotherms of the first heating process. The  $T_m$  was taken as the peak temperature. For the measurement of the glass-transition temperature ( $T_g$ ), the samples were rapidly quenched to  $-100$  °C. Samples were heated from  $-100$  to  $200$  °C at a heating rate of 20 °C/min. The  $T_g$  was taken as the midpoint of the change in heat capacity.

Wide-angle X-ray diffraction (WAXD) patterns of polyester and poly(ester–amide) samples were recorded at 23 °C on a Rigaku RINT 2500 system using a nickel-filtered Cu K $\alpha$  radiation ( $\lambda = 0.154$  nm, 40 kV, 110 mA) in the  $2\theta$  range of  $6$ – $60^\circ$  at a scanning speed of 2.0 deg/min.

## Results and Discussion

**Preparation of Monodispersed Oligoesters with Symmetric Structure.** Oligoesters were prepared by a condensation reaction of each diol with an excess of dimethyl adipate or diphenyl adipate. The products of the condensation reaction were then fractionated by supercritical fluid chromatography (SCFC), and fractions were collected on the basis of specific chain length of the oligoesters.<sup>24</sup> Figure 1A shows the SCFC elution profile of oligomers of trimethylene adipate derived from dimethyl adipate and propane-1,3-diol. Figure 2A shows the typical  $^1\text{H}$  NMR spectrum of isolated oligomers of trimethylene adipate (sample Om6). Peaks (c) (4.15 ppm), (a) (2.34 ppm), (d) (1.97 ppm), and (b) (1.66 ppm) in Figure 2A were assignable to the methylene proton resonances of propane-1,3-diol and the dimethyl adipate unit, respectively. Peak (e) (3.67 ppm) was assigned to the methyl proton at the methyl ester chain end. From the intensities of these proton resonances, the molar ratio of the adipate unit (AdO), the propane-1,3-diol unit (PrO), and the chain end (MO) for sample Om6 was calculated to be AdO/PrO/MO = 8:7:2. In the same way, the molar ratios of AdO, PrO, and MO for other fractionated oligoesters were calculated, and the values were as follows: AdO/PrO/MO = 3:2:2 (sample Om1), 4:3:2 (Om2), 5:4:2 (Om3), 6:5:2 (Om4), 7:6:2 (Om5), and 9:8:2 (Om7). From these results, it was confirmed that each oligoester had a symmetric structure with adipate methyl ester end groups. Similarly, the molar ratios for fractionated oligomers of tetramethylene adipate derived from dimethyl adipate and butane-1,4-diol were calculated, and the sequential length and structure of each oligoester were characterized.

Figure 1B shows the SCFC elution profile of oligomers of trimethylene adipate derived from diphenyl adipate and propane-1,3-diol. Figure 2B shows the typical  $^1\text{H}$  NMR spectrum of isolated oligomers of trimethylene adipate (sample Op6). In Figure 2B, peaks (c) (4.15 ppm), (d) (1.97 ppm), (a) (2.33 ppm), and (b) (1.66 ppm) were similarly assignable to the methylene proton resonances of propane-1,3-diol and the adipate unit, respectively. Peak (e) (2.39 ppm), (f) (g) (1.77–1.79 ppm), (h) (2.59 ppm), and (i, j, k) (7.07–7.37 ppm) were assigned to the methylene protons and the phenyl protons at the adipate phenyl ester end group, respectively. On the basis of these peak intensities, the molar ratios of each unit were calculated, and it was confirmed that each oligoester had a defined chain length and a symmetric structure constituted of adipate phenyl ester end groups (samples Op1–7 in Figure 1B). In a similar manner, all of the fractionated oligomers of pentamethylene adipate and

hexamethylene adipate derived from diphenyl adipate and each diol were characterized.

For the confirmation of purity and structure of fractionated oligoesters, MALDI-ToF MS analysis and the reinjection analysis of the samples in SCFC were also applied. As shown in Figure 1C, the SCFC elution profile of the fractionated oligoester reinjected revealed a single peak at the identical retention time with the collected fraction in a mixture of oligomers. Furthermore, in the MALDI-ToF MS spectra of the fractionated oligoesters, the characteristic signal of ionomer with the relevant mass corresponding to the chemical structure assigned from  $^1\text{H}$  NMR was detected (data not shown). From these results, it was confirmed similarly that the oligoesters could be obtained with very high purity. However, some oligoesters, especially with long chain length derived from dimethyl adipate and diols, had comparatively low purity due to the impurities with hydroxyl end group, whereas few hydroxyl end groups were detected in the case of oligoesters derived from diphenyl adipate and diols (see Figure 2). In fact, the peaks of some samples reinjected in SCFC had slight tailing or shoulder corresponding to the small peaks between main peaks, and small amounts of these impurities were also detected as the asymmetric oligoesters by MALDI-ToF MS spectroscopy.

**Copolymerization of Monodispersed Oligoesters with Butane-1,4-diamines.** The reaction of the obtained monodispersed oligoesters with butane-1,4-diamine was carried out in the absence of catalyst at 120 °C for 6 h under nitrogen. The mixtures of oligoesters and diamine were in a molten state at the initial stage of reaction, but as the condensation reaction progressed, the viscosity of the mixture increased. For the mixtures of oligomers of tetramethylene adipate with butane-1,4-diamine, the reaction phase transformed to a solid state. In contrast, for the mixtures of butane-1,4-diamine and oligomers of trimethylene adipate with methyl ester end groups, the reaction phase was nearly unchanged during the condensation reaction at 120 °C for 6 h, and few polymeric products were obtained after the reaction in any cases. In the absence of catalyst, the methyl ester end groups may have relatively low activity for the amidation reaction under the conditions of the molten state. In addition, a fraction of butane-1,4-diamine evaporated from the reaction solution during the polymerization reaction; thus, the chain extension reaction may be inefficient under these conditions. To improve the amidation activity between oligoesters and butane-1,4-diamine, the oligomers of trimethylene adipate with nucleophilic phenyl ester end groups were used as macromonomers.<sup>27</sup> By using the oligomers of trimethylene adipate with phenyl ester end groups, the polymerization reactions with butane-1,4-diamine progressed very fast, and the viscosity of the mixture radically increased in a short time. In a similar manner, we could obtain the polymeric products from the monodispersed oligomers of pentamethylene adipate phenyl ester and of hexamethylene adipate phenyl ester with butane-1,4-diamine.

Table 1 lists the results of the polymerization of monodispersed oligoesters with butane-1,4-diamine. Four series of copolymers from trimethylene adipate and butane-1,4-diamine (P(tri)), from tetramethylene adipate and butane-1,4-diamine (P(tet)), from pentamethylene adipate and butane-1,4-diamine (P(pen)), and from hexamethylene adipate and butane-1,4-diamine (P(hex)) were obtained from monodispersed oligoesters with different repeating units in satisfactory yields (56–89%). The obtained copolymers were characterized by  $^1\text{H}$  and  $^{13}\text{C}$  NMR analyses. Figure 3 shows the typical  $^1\text{H}$  and  $^{13}\text{C}$  NMR spectra of the products from the condensation reaction of the

Table 1. Polymerization Results, Compositions, and Molecular Weights of Periodic Copolymers and Homopolyesters

sample no.	macromonomer (ester unit)	sequential no. of ester unit	polymer yield (%)	amide fraction		molecular weight <sup>b</sup>	
				mol % (theortl)	mol % <sup>a</sup> (expl)	$M_n$	$M_w/M_n$
P(tri)1	trimethylene adipate	2	66	33	34	— <sup>c</sup>	—
P(tri)2		3	79	25	26	—	—
P(tri)3		4	82	20	20	—	—
P(tri)4		5	76	17	17	10 300	2.3
P(tri)5		6	74	14	14	18 400	2.1
P(tri)6		7	68	13	13	14 000	2.4
P(tri)7		8	69	11	11	17 200	2.2
P(tet)1	tetramethylene adipate	2	68	33	34	—	—
P(tet)2		3	62	25	26	—	—
P(tet)3		4	67	20	20	—	—
P(tet)4		5	63	17	17	15 200	2.6
P(tet)5		6	71	14	15	12 800	2.2
P(tet)6		7	56	13	13	14 000	2.4
P(pen)1	pentamethylene adipate	2	80	33	33	—	—
P(pen)2		3	84	25	25	—	—
P(pen)3		4	81	20	20	—	—
P(pen)4		5	75	17	16	15 700	2.0
P(pen)5		6	81	14	14	22 300	2.0
P(pen)6		7	79	13	12	22 700	2.0
P(pen)7		8	68	11	11	24 100	2.0
P(hex)1	hexamethylene adipate	2	83	33	34	—	—
P(hex)2		3	79	25	26	—	—
P(hex)3		4	68	20	21	—	—
P(hex)4		5	73	17	17	10 700	2.2
P(hex)5		6	63	14	15	13 100	2.1
P(hex)6		7	89	13	12	18 900	2.1
P(hex)7		8	76	11	11	14 000	2.0
	poly(trimethylene adipate)		74	0	0	18 500	1.5
	poly(tetramethylene adipate)		81	0	0	17 000	1.8
	poly(pentamethylene adipate)		83	0	0	14 200	1.5
	poly(hexamethylene adipate)		69	0	0	22 800	1.4

<sup>a</sup> Determined from <sup>1</sup>H NMR spectra. <sup>b</sup> Determined by GPC analysis. <sup>c</sup> Not determined.

monodispersed oligomer of trimethylene adipate (sample Op6) and butane-1,4-diamine. As shown in Figure 3A, the methylene proton signals and phenyl proton signals arising from adipate phenyl ester end group (peaks (e) to (k) in Figure 2B) completely disappeared in the <sup>1</sup>H NMR spectrum, and new peaks at 1.53, 1.66, 2.20, and 3.26 ppm were detected in addition to the methylene proton signals corresponding to the trimethylene adipate units (peaks (a) to (d) in Figures 2B and 3A). Peaks (e) (1.66 ppm) and (f) (2.20 ppm) were assigned to the methylene protons of adipamic acid units. Peaks (g) (3.26 ppm) and (h) (1.53 ppm) were assignable to the methylene protons of butane-1,4-diamine units. No proton signals corresponding to the adipamide units were detected in the <sup>1</sup>H NMR spectra of any of the products. From the peak intensities of the methylene protons of adipate unit (AdO), propane-1,3-diol unit (PrO), adipamic acid unit (AdN), and butane-1,4-diamine (BuN), the molar ratio of AdO, PrO, AdN, and BuN for sample P(tri)6 was calculated to be AdO/PrO/AdN/BuN = 6:7:2:1. The molar ratios of AdO, PrO, AdN, and BuN for the other produced copolymers were also calculated from their respective peak intensities as follows: AdO/PrO/AdN/BuN = 1:2:2:1 (sample P(tri)1), 2:3:2:1 (P(tri)2), 3:4:2:1 (P(tri)3), 4:5:2:1 (P(tri)4), 5:6:2:1 (P(tri)5), and 7:8:2:1 (P(tri)7). From these results, it has been concluded that the amidation between the ester chain ends of oligoesters and butane-1,4-diamine progressed selectively and that the produced copolymers have a periodical sequence corresponding to the sequential length of the initial monodispersed oligoesters. Actually, as shown in Figure 3B, the distinct and simple peaks, not complex, were observed in the <sup>13</sup>C NMR spectra for peaks (i) to (k) (CO: 173–174 ppm), (c) (OCH<sub>2</sub>: 61 ppm), (g) (NHCH<sub>2</sub>: 39 ppm), and (a) and (f) (OCOCH<sub>2</sub> and NHCOCH<sub>2</sub>: 37–33 ppm), which were sensitive for the neighboring molecular structures, indicating that the identical ester–amide sequences were present with high regularity in the

produced copolymers. All of the copolymers synthesized by polycondensation reaction of monodispersed oligomers of tetra-, penta-, and hexamethylene adipate with butane-1,4-diamine were similarly characterized on the basis of NMR analyses (see Figure 4A–C), and it was confirmed that the produced copolymers had defined periodic sequences consisting of amides and esters from each groups (Scheme 1 and Table 1). Small signals arising from the methyl ester chain end and from hydroxyl chain end were detected in the <sup>1</sup>H and <sup>13</sup>C NMR spectra of some of the periodic copolymers derived from oligoesters with phenyl ester end groups or with methyl ester end groups, respectively (see Figures 3 and 4). These signals originated from the oligoesters with an asymmetric structure consisting of methyl ester end groups and hydroxyl end groups left as impurities after the polycondensation reaction, as mentioned above. These small amounts of oligoesters with the asymmetric structure may cause the termination or slow the progress of the chain polymerization due to low activity during the polycondensation reaction of oligoester with diamine. However, there was little loss of periodicity or uniformity of the sequential structure in the produced copolymers (see Table 1).

The products obtained from monodispersed oligoesters with short sequential lengths ranging from 2 to 4 repeating units could be dissolved in trifluoroethanol, but not in chloroform. This contrasts to the products obtained from monodispersed oligoesters with long sequential lengths ranging from 5 to 8 repeating units which were soluble in chloroform. The difference of solubility resulted from the amide group hydrogen bonds which is directly related to the periodicity and content of the comonomer. The flexibility of solvent use facilitated by hydrogen bonding in these copolymers makes these materials potentially interesting for a wide range of application in fibers and films.

Table 2. Thermal Properties and X-ray Crystallinities of Periodic Copolymers and Homopolyesters

sample no.	sequential no. of ester unit	amide fraction	thermal properties <sup>a</sup>					
		mol % (theoretical)	$T_g/^\circ\text{C}$	$T_m/^\circ\text{C}$	$\Delta H_m/\text{J g}^{-1}$	$T_{m2}/^\circ\text{C}$	$\Delta H_{m2}/\text{J g}^{-1}$	$X_c^{b}/\%$
P(tri)1	2	33	−29	84	7	120	2	19
P(tri)2	3	25	−41	76	21	108	10	25
P(tri)3	4	20	−47	72	22	—	—	26
P(tri)4	5	17	−51	68	24	—	—	22
P(tri)5	6	14	−52	62	26	—	—	22
P(tri)6	7	13	−55	63	23	—	—	19
P(tri)7	8	11	−56	62	31	—	—	19
P(tet)1	2	33	− <sup>c</sup>	258	31	—	—	33
P(tet)2	3	25	—	255	25	—	—	38
P(tet)3	4	20	—	245	26	—	—	29
P(tet)4	5	17	—	241	19	—	—	25
P(tet)5	6	14	—	221	20	—	—	26
P(tet)6	7	13	—	209	18	—	—	28
P(pen)1	2	33	−37	91	13	—	—	22
P(pen)2	3	25	−45	67	19	—	—	18
P(pen)3	4	20	−49	57	17	—	—	20
P(pen)4	5	17	−55	54	20	—	—	20
P(pen)5	6	14	−59	49	19	—	—	19
P(pen)6	7	13	−61	47	24	—	—	25
P(pen)7	8	11	−61	45	23	—	—	24
P(hex)1	2	33	−40	74	6	102	2	16
P(hex)2	3	25	−50	68	10	—	—	14
P(hex)3	4	20	−53	62	11	—	—	19
P(hex)4	5	17	−57	58	17	—	—	22
P(hex)5	6	14	−57	55	12	—	—	19
P(hex)6	7	13	−60	56	38	—	—	27
P(hex)7	8	11	−59	56	39	—	—	26
poly(trimethylene adipate)		0	−63	40	33	—	—	33
poly(tetramethylene adipate)		0	−58	62	52	—	—	60
poly(pentamethylene adipate)		0	−73	40	50	—	—	39
poly(hexamethylene adipate)		0	−69	55	58	—	—	39

<sup>a</sup> Measured by DSC. <sup>b</sup> Crystallinities determined from X-ray diffraction patterns. <sup>c</sup> Not determined.

For the produced periodic copolymers, the molecular weights ( $M_n$ ) and polydispersity indices ( $M_w/M_n$ ) of chloroform-soluble samples were determined from GPC analysis and ranged from 10 300 to 24 100 and from 2.0 to 2.6 compared to a polystyrene standard, respectively.

**Thermal Properties of Periodic Poly(ester–amide)s.** Glass-transition temperatures ( $T_g$ ), melting temperatures ( $T_m$ ), and heats of fusion ( $\Delta H_m$ ) of copolymer samples were determined from DSC measurements. The results are listed in Table 2, together with the data of homopolyesters. The  $T_m$  values of the periodic poly(ester–amide)s were higher than those of homopolyesters composed of the same ester units and tended to increase with an increase in amide content. The  $T_m$  values of P(tet) series were measured at over 200 °C and were remarkably higher than the  $T_m$  (62 °C) of the poly(tetramethylene adipate) homopolyester. Although the improved temperatures ranges were lower than those of P(tet) series, a similar trend was observed on the  $T_m$  values of P(tri) series, and the copolymer sample with lowest amide content also showed high thermal stability ( $T_m = 62$  °C) as compared with the poly(trimethylene adipate) homopolyester ( $T_m = 40$  °C) (Figure 5). On the other hand, the  $T_m$  values of both P(pen) and P(hex) series showed a slight increase with increasing the amide content, while no great difference of the  $T_m$  values was observed between copolymer samples with amide content less than 17 mol % and homopolyesters (Table 2 and Figure 5). In addition, for the P(tri) and P(hex) series, some copolymer samples showed two distinct melting peaks (samples P(tri)1, 2 and P(hex)1 in Table 2).

In the DSC thermograms for the P(tri), P(pen), and P(hex) samples, the change in heat capacity corresponding to the glass-transition phenomenon could be detected, and the  $T_g$  values of the periodic poly(ester–amide)s also tended to increase with an increase in the amide content. However, the  $T_g$  could not be

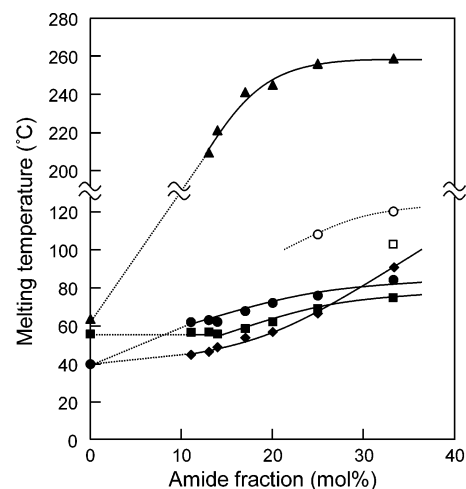


**Figure 5.** Melting temperatures of the periodic poly(ester–amide)s as a function of amide unit fraction, P(tri) series (●,  $T_{m1}$ ; ○,  $T_{m2}$ ), P(tet) series (▲), P(pen) series (◆), P(hex) series (■,  $T_{m1}$ ; □,  $T_{m2}$ ). The symbols at the 0 mol % amide fraction show the  $T_m$  values of homopolyesters.

detected in the DSC thermograms for P(tet) copolymer series, since the crystallization occurred during the cooling process from the melt state at over 200 °C.

Plots of the  $T_m$  values of periodic poly(ester–amide)s with each amide unit content as a function of the number of methylene groups in the diol units for oligoesters revealed high  $T_m$  values for the samples with an even number of methylene groups and low  $T_m$  values for the samples with an odd number of methylene groups (Figure 6). Such behavior, the so-called “odd–even effect”, has been reported previously for polyamides,<sup>28–30</sup> polyurethanes,<sup>31,32</sup> poly(ester–amide)s,<sup>20,33,34</sup> poly-



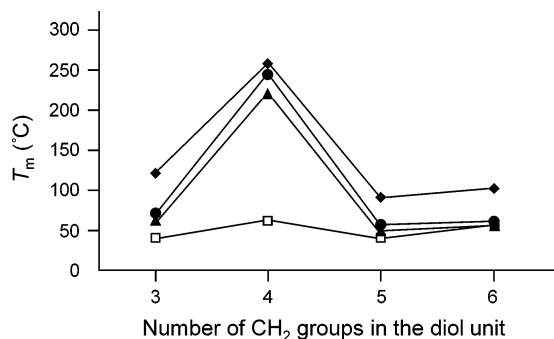


**Figure 6.** Melting temperatures of the periodic poly(ester–amide)s with 33 mol % amide unit content (◆), 20 mol % amide unit content (●), and 14 mol % amide unit content (▲) and of homopolyesters (□) as a function of the number of CH<sub>2</sub> groups in the diol unit.

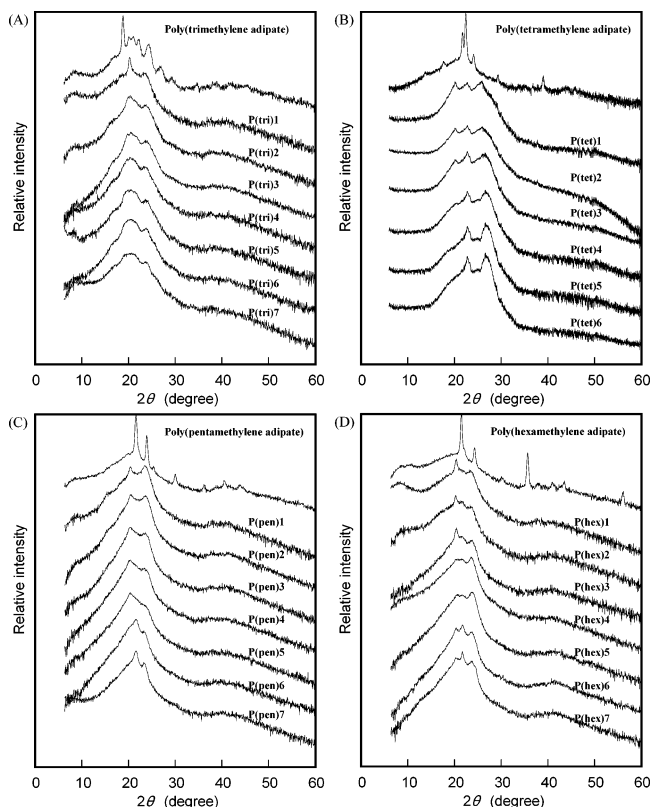


**Figure 7.** X-ray diffraction patterns of periodic copolymers and homopolyesters: (A) samples P(tri)1–7 and poly(trimethylene adipate), (B) samples P(tet)1–6 and poly(tetramethylene adipate), (C) samples P(pen)1–7 and poly(pentamethylene adipate), and (D) samples P(hex)1–7 and poly(hexamethylene adipate).

(amide–urethane)s,<sup>27,35</sup> and poly(urea–urethane)s.<sup>37</sup> However, it is of interest to note that the odd–even effect for periodic poly(ester–amide)s is only dependent on the number of methylene groups in the diol units as comonomers, but not on the defined sequential number of ester units.

**X-ray Diffraction Patterns of Periodic Poly(ester–amide)s.** The wide-angle X-ray diffraction (WAXD) patterns of periodic poly(ester–amide)s were recorded. Figure 7 shows the WAXD patterns of all of the periodic poly(ester–amide)s, together with the WAXD patterns of homopolyesters. The crystalline structures of poly(tetramethylene adipate)<sup>38–40</sup> and poly(hexamethylene adipate)<sup>41</sup> were previously investigated, and both diffraction patterns showed the reflections arising from each orthorhombic unit cell. In the diffraction diagrams of poly(tetramethylene adipate) and poly(hexamethylene adipate), two main diffraction peaks located at  $2\theta$  values of 22.1° and 23.9° and

of 21.2° and 24.0° were assignable to (020) and (021) planes and to (210) and (020) planes, respectively (Figure 7B,D). Unfortunately, the crystalline structures of poly(trimethylene adipate) and poly(pentamethylene adipate) have not been characterized. However, several main diffraction peaks were distinctly observed in each diagram (Figure 7A,C).

In the case of P(tet) copolymers, all samples revealed different WAXD patterns as compared to poly(tetramethylene adipate), and two main peaks at  $2\theta$  values of about 23° and 26° were detected in the diffractograms. Although the P(tri) copolymers gave relatively broad diffraction peaks, the diffraction patterns differed from that of poly(trimethylene adipate). Since the crystalline structures of the periodic poly(ester–amide)s have not been defined, further research is needed for the understanding of the relation between the thermal properties and crystalline structures. However, these results strongly suggest that the amide units introduced periodically into the polyester main chains are included in the crystalline region to form a different chain packing structure as compared to the homopolyesters. The differences in chain packing structure lead to an increase in the  $T_m$  values of periodic copolymers as compared with the homopolyesters, and the amide units in the crystalline region may form intermolecular hydrogen bond interactions.

Unlike the P(tet) and P(tri) copolymers, the diffraction patterns of both P(pen) and P(hex) copolymers were strongly dependent on the amide content, and the copolymer samples with an amide content of more than 20 mol % gave different WAXD patterns from those of homopolyesters, whereas the diffraction peaks had nearly identical  $2\theta$  values as compared to the homopolyesters when the amide content of the copolymers was less than 13 mol %. Such differences in the WAXD patterns strongly correlated to the thermal behavior determined from DSC measurements. As shown in Figure 5, the P(pen) and P(hex) copolymers with more than 20 mol % amide content had apparently higher  $T_m$  values, but copolymers with less than 13 mol % amide content showed little change in  $T_m$  values as compared to the homopolyesters. As the ester sequences become longer, the formation of crystals based on these intervals may occur since the P(pen) and P(hex) copolymers have longer repeating ester units as compared with P(tri) and P(tet) copolymers.

To understand the differences in the melting property and crystalline structure among four series of copolymer samples, the possible chain arrangements of periodical ester–amide sequences were considered on the basis of molecular chain structure and their intermolecular interactions. Figure 8 shows the schematic illustration of the speculated chain arrangements for P(tri) and P(tet) copolymers. In this model, all of the molecular chains are drawn as a planar zigzag structure. The molecular chains of periodic copolymers can arrange into four main types dependent on the intermolecular hydrogen bond interactions (between amide–amide groups for type I and III and between amide–ester groups for type II and IV) and on molecular chain directions (parallel chains for type I and II and antiparallel chains for type III and IV), as shown in Figure 8. It can be expected that the periodic copolymers mainly form the chain arrangements of type II and IV rather than type I and III, since the amide unit is a minor component compared with ester unit. In addition, it has been reported that the many types of polyamides and polyesters generally form antiparallel arrangements in the stable crystalline state.<sup>42</sup> Therefore, it is proposed that type IV may be preferable to type II. As shown in Figure 8A, P(tet) copolymers can form excellent interchain arrangements based on the intermolecular hydrogen bond



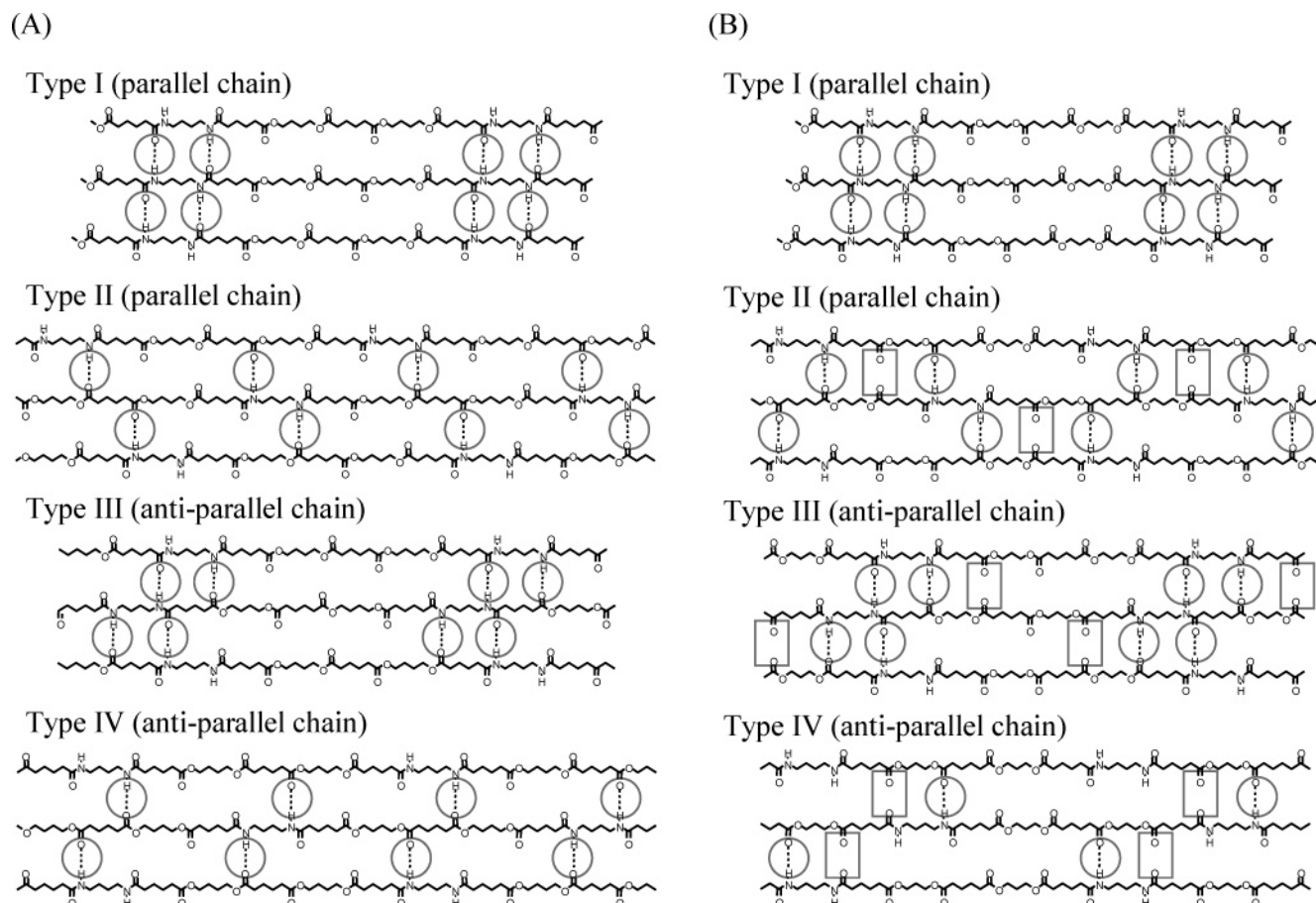


**Figure 8.** Schematic illustration of the speculated chain arrangements for periodic poly(ester–amide)s: (A) P(tet) series and (B) P(tri) series (O, intermolecular hydrogen bond interaction; □, steric hindrance).

interactions, which may lead to the higher thermal stability. However, for P(tri) copolymers, the formation of intermolecular hydrogen bond induces the steric hindrance of carbonyl groups between adjacent chains in the cases of type II, III, and IV, and conformational rearrangements must occur to form stable chain-packing structures. Furthermore, the number of the hydrogen bonds was limited in the case of type IV as compared with the other types (Figure 8B). Therefore, for the P(tri) copolymers, the chain arrangements with less-effective intermolecular hydrogen bond interactions may form and result in the slight improvement of the thermal properties. As a result, the P(tri) copolymers revealed relatively broad X-ray diffraction patterns. A similar model for interchain interaction must be applied to P(pen) series with an odd number of methylene groups, and the  $T_m$  values of P(pen) copolymers were much lower than those of P(tet) copolymers (Figure 5). Surprisingly, the  $T_m$  values of P(hex) copolymers with an even number of methylene groups also revealed lower values compared to those of P(tet) copolymers, even though the P(hex) copolymers can form the intermolecular hydrogen bond interactions without steric hindrance of carbonyl groups. This result suggests that the significant differences in thermal stability of the crystalline phase of periodic copolymers could not simply be explained in terms of the intermolecular interactions of the molecular chain arrangements. Because the P(hex) copolymers have longer repeating ester units, the crystals may be formed by the interaction between the repeating ester units rather than by the formation of intermolecular hydrogen bonds.

**Melting Behavior of Periodic Poly(ester–amide)s.** Some copolymer samples, especially for P(tri) copolymers, showed two distinct melting peaks with a temperature interval close to

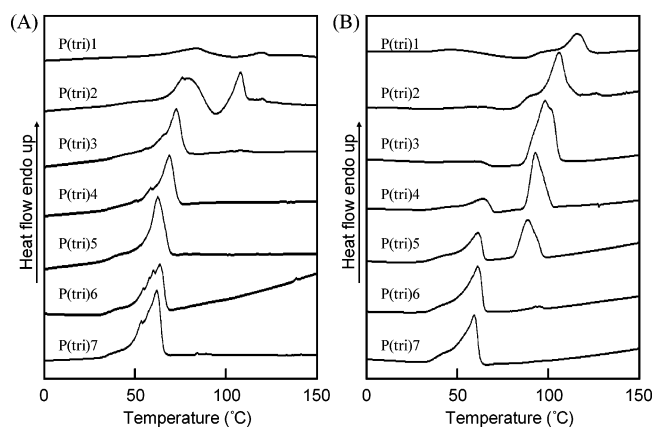
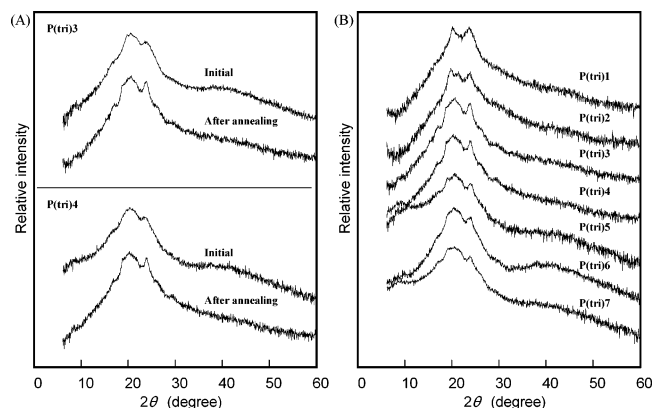
30 °C (see Table 2), and the values of both the lower  $T_m$  and higher  $T_m$  were much higher than that of the homopolymer. To obtain a further understanding of the relationship between the melting behavior and crystalline morphology, the effects of annealing on the  $T_m$  values were investigated. Copolymer samples of P(tri) series were selected, and the thermal properties of the samples annealed at 75 °C for 2 days were characterized by DSC. The results are listed in Table 3. Figure 9 shows the typical melting curves of P(tri) series before and after annealing treatment. Samples P(tri)1 and P(tri)2 initially had two endothermic peaks, while the lower  $T_m$  peaks were completely disappeared after annealing treatment. For the annealed samples P(tri)3–5, new large peaks were obviously detected, ~30 °C higher than samples that were not annealed, and the lower  $T_m$  peaks became much smaller than those of the initial samples. On the other hand, samples P(tri)6 and P(tri)7 showed little change in the melting curves before and after annealing treatment. The  $\Delta H_m$  values of annealed samples slightly increased as compared with those of the initial samples.

It has been reported that the poly(tetramethylene adipate) revealed the temperature-induced polymorphism phenomenon, since poly(tetramethylene adipate) forms the  $\beta$  crystal (orthorhombic unit cell with  $a = 0.506$  nm,  $b = 0.735$  nm, and  $c = 1.467$  nm) at temperatures region below 27 °C, while the  $\alpha$  crystal (monoclinic unit cell with  $a = 0.673$  nm,  $b = 0.794$  nm,  $c = 1.420$  nm, and  $\beta = 45.5^\circ$ ) is generated at temperatures region above 32 °C.<sup>38–40,43</sup> In the poly(tetramethylene adipate) samples crystallized at temperatures ranging from 27 to 32 °C,  $\alpha$  and  $\beta$  crystals coexist, and the samples revealed distinct two melting peaks corresponding to each crystalline morphism. The WAXD patterns of annealed P(tri) samples were recorded in

**Table 3.** Melting Temperatures and Crystallinities of Periodic Copolymer P(tri) Series before and after Annealing

sample no.	sequential no. of ester unit	initial					after annealing				
		thermal properties <sup>a</sup>					thermal properties <sup>a</sup>				
		$T_{m1}/^{\circ}\text{C}$	$\Delta H_{m1}/\text{J g}^{-1}$	$T_{m2}/^{\circ}\text{C}$	$\Delta H_{m2}/\text{J g}^{-1}$	$X_c^b/\%$	$T_{m1}/^{\circ}\text{C}$	$\Delta H_{m1}/\text{J g}^{-1}$	$T_{m2}/^{\circ}\text{C}$	$\Delta H_{m2}/\text{J g}^{-1}$	$X_c^b/\%$
P(tri)1	2	84	7	120	2	19	—	—	115	12	21
P(tri)2	3	76	21	108	10	25	—	—	105	22	21
P(tri)3	4	72	22	—	—	26	—	—	98	30	28
P(tri)4	5	68	24	—	—	22	64	8	93	19	25
P(tri)5	6	62	26	—	—	22	61	14	88	15	22
P(tri)6	7	63	23	—	—	19	61	22	—	—	24
P(tri)7	8	62	31	—	—	19	59	22	—	—	18

<sup>a</sup> Measured by DSC. <sup>b</sup> Crystallinities determined from X-ray diffraction patterns.

**Figure 9.** Melting curves of periodic poly(ester-amide)s (samples P(tri) series): (A) before annealing and (B) after annealing at 75 °C for 2 days.**Figure 10.** X-ray diffraction patterns of periodic poly(ester-amide)s: (A) samples P(tri)3 and P(tri)4 before and after annealing treatment; (B) all P(tri) samples after annealing treatment.

order to examine whether the different melting peaks arise from a polymorphism phenomenon. Figure 10 shows the WAXD patterns of the annealed samples P(tri)1–7. The diffraction patterns of the annealed samples P(tri)3 and P(tri)4 which showed the drastic change in the DSC curves became slightly sharp as compared with initial states (Figure 10A). However, two main peaks located at  $2\theta$  values of about  $20^{\circ}$  and  $24^{\circ}$  were detected on both the initial and annealed samples, and only slight differences of WAXD patterns were observed (see Figures 7 and 10), indicating that the crystalline structures of the initial and annealed samples are identical. Recently, similar thermal behaviors have been reported for the segmented poly(ester-amide)s containing the ester and amide blocks derived from bisamide-diols,<sup>25,26</sup> and as a results of DSC and FT-IR analysis, it was concluded that the two distinct melting temperatures of the copolymers, dependent on the content of the amide blocks, were ascribed to the melting of crystals comprising single ester-

amide sequences or two or more ester-amide sequences. On the basis of the above results, considering the drastic change of the  $T_m$  values, the following two possible models are proposed on the annealing effect of the periodic polyester-amides; one is that the molecular chain rearrangement takes place to reduce the crystalline defects such as steric hindrance of carbonyl groups without changing the crystalline structure, and the other is that the numbers of amide units included in the crystalline region increase by the thickening of lamellar during crystallization.

## Conclusions

Novel copolymers with a periodic sequence structure consisting of ester and amide groups could be synthesized by two-step polycondensation reactions from adipate, butane-1,4-diamine, and linear aliphatic diols consisting of both odd and even methylene groups. The thermal properties of the obtained periodic poly(ester-amide) series were strongly dependent on both the monomeric and sequential structures, and the values could be regulated over a wide temperature range. The WAXD patterns of periodic poly(ester-amide)s also varied with the monomeric and sequential structures, suggesting that the molecular chain arrangements based on the periodic ester-amide sequence and their intermolecular hydrogen bond interactions are important factors for the formation of a thermally stable crystalline region. Moreover, from the results of the WAXD patterns and DSC curves observed for periodic poly(ester-amide) samples before and after annealing treatment, it has been found that the crystalline region, including the amide unit, transforms to a more stable state during the annealing treatment by either the rearrangement of the molecular chains or an increase in lamellar thickness.

**Acknowledgment.** We appreciate the assistance provided by Dr. C. T. Nomura for the critical reading our manuscript and by Dr. N. Dohmae for MALDI MS spectroscopy measurement. This work was supported by a Grant-in-Aid for Young Scientists (B) from the Ministry of Education, Culture, Sports, Science and Technology of Japan (No. 17750147) (to H.A.) and in part by a grant for Ecomolecular Science Research from RIKEN Institute.

## References and Notes

- (1) Lee, S. Y.; Park, S. H.; Hong, S. H.; Lee, Y.; Lee, S. H. In *Biopolymers*; Doi, Y., Steinbüchel, A., Eds.; VCH-Wiley: Weinheim, 2001; Vol. 3b, p 265.
- (2) Lee, S. Y.; Hong, S. H.; Lee, S. H.; Park, S. J. *Macromol. Biosci.* **2004**, *4*, 157–164.
- (3) Katayama, S.; Murakami, T.; Takahashi, Y.; Serita, H.; Obuchi, Y.; Ito, Y. *J. Appl. Polym. Sci.* **1976**, *20*, 975–994.
- (4) Tokiwa, Y.; Suzuki, T.; Ando, T. *J. Appl. Polym. Sci.* **1979**, *24*, 1701–1711.
- (5) Castaldo, L.; de Candia, F.; Maglio, G.; Palumbo, R.; Strazza, G. *J. Appl. Polym. Sci.* **1982**, *27*, 1809–1822.

- (6) Goodman, I.; Sheahan, R. J. *Eur. Polym. J.* **1990**, *26*, 1081–1088.
- (7) Inata, H.; Matsumura, S. *J. Appl. Polym. Sci.* **1985**, *30*, 3325–3337.
- (8) Seppälä, J. V.; Helminen, A. O.; Korhonen, H. *Macromol. Biosci.* **2004**, *4*, 208–217.
- (9) Gonsalves, K. E.; Chen, X.; Cameron, J. *Macromolecules* **1992**, *25*, 3309–3312.
- (10) Bera, S.; Jedlinski, Z. *J. Polym. Sci., Part A: Polym. Chem.* **1993**, *31*, 731–739.
- (11) Nagata, M.; Kiyotsukuri, T. *Eur. Polym. J.* **1994**, *30*, 1277–1281.
- (12) Arvanitoyannis, I.; Nakayama, A.; Kawasaki, N.; Yamamoto, N. *Polymer* **1995**, *36*, 857–866.
- (13) Alla, A.; Rodriguez-Galan, A.; Martinez de Ilarduya, A.; Munoz-Guerra, S. *Polymer* **1997**, *38*, 4935–4944.
- (14) Villuendas, I.; Molina, I.; Regano, C.; Bueno, M.; Martinez de Ilarduya, A.; Galbis, J. A.; Munoz-Guerra, S. *Macromolecules* **1999**, *32*, 8033–8040.
- (15) Stapert, H. R.; Bouwens, A.-M.; Dijkstra, P. J.; Feijen, J. *Macromol. Chem. Phys.* **1999**, *200*, 1921–1929.
- (16) Dijkstra, P. J.; Stapert, H. R.; Feijen, J. *Macromol. Symp.* **2000**, *152*, 127–137.
- (17) Tuominen, J.; Seppälä, J. V. *Macromolecules* **2000**, *33*, 3530–3535.
- (18) Villuendas, I.; Bou, J. J.; Rodriguez-Galan, A.; Munoz-Guerra, S. *Macromol. Chem. Phys.* **2001**, *202*, 236–244.
- (19) Asin, L.; Armelin, E.; Montane, J.; Rodriguez-Galan, A.; Puiggali, J. *J. Polym. Sci., Part A: Polym. Chem.* **2001**, *39*, 4283–4293.
- (20) Fey, T.; Keul, H.; Höcker, H. *Macromol. Chem. Phys.* **2003**, *204*, 591–599.
- (21) Rodriguez-Galan, A.; Vera, M.; Jimenez, K.; Franco, L.; Puiggali, J. *Macromol. Chem. Phys.* **2003**, *204*, 2078–2089.
- (22) Ferré, T.; Franco, L.; Rodriguez-Galan, A.; Puiggali, J. *Polymer* **2003**, *44*, 6139–6152.
- (23) Vera, M.; Almontassir, A.; Rodriguez-Galan, A.; Puiggali, J. *Macromolecules* **2003**, *36*, 9784–9796.
- (24) Abe, H.; Doi, Y. *Macromol. Rapid Commun.* **2004**, *25*, 1303–1308.
- (25) Lips, P. A. M.; Broos, R.; van Heeringen, M. J. M.; Dijkstra, P. J.; Feijen, J. *Polymer* **2005**, *46*, 7823–7833.
- (26) Lips, P. A. M.; Broos, R.; van Heeringen, M. J. M.; Dijkstra, P. J.; Feijen, J. *Polymer* **2005**, *46*, 7834–7842.
- (27) For example, see: Sharama, B.; Ubaghs, L.; Keul, H.; Höcker, H.; Loontjens, T.; van Benthem, R. *Macromol. Chem. Phys.* **2004**, *205*, 1536–1546.
- (28) Franco, L.; Navarro, E.; Subirana, J. A.; Puiggali, J. *Macromolecules* **1994**, *27*, 4284–4297.
- (29) Bennett, C.; Mathias, L. J. *J. Polym. Sci., Part A: Polym. Chem.* **2005**, *43*, 936–945.
- (30) Villaseñor, P.; Franco, L.; Subirana, J. A.; Puiggali, J. *J. Polym. Sci., Part B: Polym. Phys.* **1999**, *37*, 2383–2395.
- (31) Versteegen, R. M.; Sijbesma, R. P.; Meijer, E. W. *Angew. Chem., Int. Ed.* **1999**, *38*, 2917–2919.
- (32) Neffgen, S.; Kušan, J.; Fey, T.; Keul, H.; Höcker, H. *Macromol. Chem. Phys.* **2000**, *201*, 2108–2114.
- (33) Serrano, P. J.; van Duynhoven, J. P. M.; Gaymans, R. J.; Hulst, R. *Macromolecules* **2002**, *35*, 8013–8019.
- (34) Husken, D.; Krijgsman, J.; Gaymans, R. J. *Polymer* **2004**, *45*, 4837–4843.
- (35) Sharama, B.; Ubaghs, L.; Keul, H.; Höcker, H.; Loontjens, T.; Van Benthem, R. *Polymer* **2004**, *45*, 5427–5440.
- (36) Laco, J. I. I. *Polymer* **2004**, *45*, 7025–7033.
- (37) Ubaghs, L.; Keul, H.; Höcker, H. *Polymer* **2005**, *46*, 1459–1465.
- (38) Minke, R.; Blackwell, J. J. *Macromol. Sci., Phys.* **1979**, *B16*, 407–417.
- (39) Minke, R.; Blackwell, J. J. *Macromol. Sci., Phys.* **1980**, *B18*, 233–255.
- (40) Iwata, T.; Kobayashi, S.; Tabata, K.; Yonezawa, N.; Doi, Y. *Macromol. Biosci.* **2004**, *4*, 296–307.
- (41) Aylwin, P. A.; Boyd, R. H. *Polymer* **1984**, *25*, 323–329.
- (42) For example, see: Atkins, E.; Hill, M.; Hong, S. K.; Keller, A.; Organ, S. *Macromolecules* **1992**, *25*, 917–924. Johnson, C. G.; Cypcar, C. C.; Mathias, L. J. *Macromolecules* **1995**, *28*, 8535–8540. Bermúdez, M.; León, S.; Alemán, C.; Muñoz-Guerra, S. *J. Polym. Sci., Part B: Polym. Phys.* **2000**, *38*, 41–52. Bermúdez, M.; León, S.; Alemán, C.; Muñoz-Guerra, S. *Polymer* **2000**, *41*, 8961–8973. Furuhashi, Y.; Iwata, T.; Sikorski, P.; Atkins, E.; Doi, Y. *Macromolecules* **2000**, *33*, 9423–9431. Furuhashi, Y.; Sikorski, P.; Atkins, E.; Iwata, T.; Doi, Y. *J. Polym. Sci., Part B: Polym. Phys.* **2001**, *39*, 2622–2634.
- (43) Gan, Z.; Abe, H.; Doi, Y. *Macromol. Chem. Phys.* **2002**, *203*, 2369–2374.

MA052566J